Intensity measurements of low energy cosmic ray muons underground

1973 J. Phys. A: Math. Nucl. Gen. 6 1960

(http://iopscience.iop.org/0301-0015/6/12/021)

J. Phys. A: Math., Nucl. Gen., Vol. 6, December 1973. Printed in Great Britain.

Intensity measurements of low energy cosmic ray muons underground

P N Bhat and P V Ramana Murthy

Tata Institute of Fundamental Research, Bombay 5, India

Received 7 May 1973

Abstract. Intensities of cosmic ray muons coming to rest in a 444 l liquid scintillator tank at depths 96, 417 and 985 hg cm^{-2} (1 hg cm^{-2} = 100 g cm^{-2} of matter underground) have been measured to be $(7{\cdot}67 \pm 0{\cdot}4) \times 10^{-6}$, $(7{\cdot}9 \pm 0{\cdot}5) \times 10^{-8}$ and $(6{\cdot}9 \pm 0{\cdot}7) \times 10^{-9}$ muons cm^{-2} s^{-1} sr^{-1} (100 g cm^{-2} of rock)$^{-1}$ respectively. Experimental details are given and the results discussed. It is concluded that the observations can be accounted for in terms of two components: (i) muons produced in the atmosphere and penetrating to the respective depths; and (ii) muons generated locally by the decays of pions which are in turn produced in the hadronic cascades initiated by high energy muons via photomeson production by the virtual and real photons associated with muons. No new process for low energy muon production is required at the depths investigated.

1. Introduction

In the past, several experiments were carried out to measure cosmic ray intensities underground as a function of depth; see, for example, George (1952) for a summary of the early experiments and Menon and Ramana Murthy (1967) for the more recent. In general, one measures the flux of charged particles, assumed with justification to be muons, that are capable of penetrating a nominal amount ($\lesssim 100$ g cm^{-2}) of absorber as a function of depth; the measurements are therefore of *integral* type. Low energy ($\lesssim$ few hundred MeV) muons form a very small percentage of all such particles at all depths, at least down to depths of the order of 3600 m of rock below which the neutrino-produced low energy muons form a sizeable fraction of all the muons. If something anomalous is happening in the processes that lead to the existence of *low energy* muon fluxes at various depths, it would hardly be revealed in the usual depth–intensity measurements. There have been very few experiments in the past in which one measured the intensities exclusively of low energy muons and among the few that there are, the agreement is not very good. We have, therefore, undertaken the present experiment to measure the intensities of low energy muons as a function of depth in a systematic way, using the same apparatus at all the depths. Preliminary results from this experiment were reported at the Hobart Conference (Bhat and Ramana Murthy 1971) and short descriptions published (Bhat and Ramana Murthy 1972, 1973). In this paper, we present the details and final results.

2. Experimental details

2.1. Apparatus and method

The experimental arrangement is shown in figure 1. It consists of two liquid scintillation (Shellsol A) detectors S_1 and S_2 separated by 2·5 cm thick layer of lead. S_1 is viewed by one photomultiplier of 5 cm diameter (RCA 6810) and S_2 by six (RCA 6810). S_1 mainly serves to define the geometry. S_2 contains 444 l (386 kg) of liquid scintillator wherein the stopping charged particles and charged decay products are seen. Since the aim is to measure the fluxes of stopping muons, it would have been logical to employ another detector below S_2 in anticoincidence. In the present arrangement such an anticoincidence counter should have had dimensions of at least 2 m × 2 m. In view of the working conditions underground and the unwieldy nature of such a large counter we did not use any anticoincidence counter.

The essentials of the electronic schematic are shown in figure 2. The S_2 signal is generated by a coincidence between two groups of photomultipliers (ABC and DEF as shown in figure 2) rather than by the sum of signals from all the six photomultipliers, essentially to reduce the S_2 rate due to photomultiplier noise and much of the background radioactivity. Each of the photomultiplier outputs (A to G) were fed to individual amplifiers; the outputs from the amplifiers were combined into three groups (ABC, DEF and G) and fed to three individual discriminators. The discriminator outputs were fed to the coincidence circuits shown in figure 2. Muons passing through the detectors S_1 and S_2 generate S_1S_2 coincidences (resolving time = 30 ns) which are delayed by 55 ns and then made to open a gate, 68 ns wide. When this first gate closes, it opens a second gate of width approximately twice that of the first. When the second gate closes it opens in turn a third gate whose width is approximately twice that of the second. In this fashion there are 10 gates in cascade whose widths are in geometrical progression with a common ratio of about 2, the width of the tenth gate being 27·2 μs. The outputs from these 10 gates are fed to 10 different two-fold coincidence circuits. The S_2 pulse is shaped (width ≃ 8 ns) and fed to each of these 10 coincidence circuits.

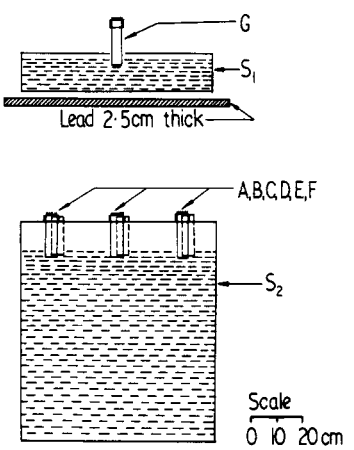

Figure 1. Experimental arrangement. A, B, C, D, E, F and G are photomultipliers; S_1 and S_2 are liquid scintillators of dimensions 76·4 × 76·4 × 12·7 cm^3 and 76·4 × 76·4 × 76·4 cm^3 respectively.

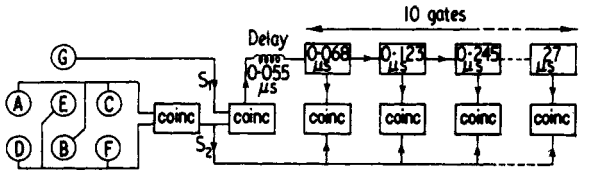

Figure 2. Block diagram of the electronics employed in the experiment.

A muon stopping in S_2, after passing through S_1, generates an S_1S_2 coincidence pulse and the decay electron, a delayed S_2 pulse. The prompt and delayed pulses produce a coincidence signal in one of the 10 gates. The time interval Δt in the two-pulse sequence (S_1S_2 and delayed S_2) is determined by the gate in which coincidence takes place. If w_i ($i = 1$ to 10) is the width of the ith gate, a coincidence output from jth channel implies that Δt lies in the interval $55\text{ ns} + \Sigma_{i=1}^{j-1} w_i$ to $55\text{ ns} + \Sigma_{i=1}^{j} w_i$ where 55 ns is the initial delay. The output of each of the 10 coincidence circuits is recorded by individual call counters; besides, each coincidence is made to light a labelled bulb (to obtain Δt) which is photographed. In addition, during part of the run, we displayed an oscilloscope and photographed information on the times of occurrence of the delayed coincidence and the end of an 8 μs gate opened by an S_1S_2 coincidence signal. This information allows us to determine Δt independently. All these results were mutually consistent.

2.2. Location of the experiment

The experiment was carried out at Kolar Gold Fields (870 m above mean sea level, 13° N geographic latitude and 78° E longitude) in India. The same apparatus was set up and observations made consecutively at the surface and at depths of 96 hg cm^{-2}, 417 hg cm^{-2} and 985 hg cm^{-2} (measured from the top of the atmosphere; 1 hg cm^{-2} = 100 g cm^{-2} of matter). At each depth, the apparatus was placed towards one wall in a long tunnel whose cross section was approximately 3 m × 3 m. Thus the roof was approximately 2 m above the S_2 scintillator.

2.3. Background radioactivity and efficiency of the apparatus

Voltages on the individual photomultipliers were set in the following way. Keeping all the amplifier gains and discriminator biases fixed, we varied the voltage on one of the photomultipliers, for example G, while maintaining the voltages on the rest of the photomultipliers constant. When we observed and plotted the S_1S_2 coincidence rate as a function of voltage on the photomultiplier G, we found a rising curve followed by a plateau. We fixed the voltage on G at a value of 50 V higher than the voltage at the onset of the plateau.

Earlier we described (§ 2.1) the two-pulse sequence in the case of stopping muons. Since we did not employ an anticoincidence counter below S_2, the gates in figure 2 are opened also by S_1S_2 pulses due to penetrating muons that go through S_2 without stopping. Since the gates are put in coincidence with S_2, one should expect chance coincidences between S_1S_2 (due to penetrating muons) and S_2. These constitute spurious background simulating stopping muons and have to be corrected for. To make the correction negligible, one has to keep S_1S_2 and S_2 rates to a minimum consistent with a near 100% efficiency for observing the μ–e decays. To meet this condition we generate the S_2 pulse, as stated earlier, as a coincidence between two pulses from

the two groups of photomultipliers viewing the same scintillator. It must be emphasized, however, that even then the background radioactivity can occasionally induce *genuine* S_2 coincidences since all of the six photomultipliers view the *same detector* in which gamma rays can produce Compton electrons. It is observed that the S_2 counting rate (at the same voltage settings on the photomultipliers and bias settings on the discriminators) is not much dependent† (2400 counts min^{-1} to 560 counts min^{-1}) on depth and, consequently, serves as a guideline to indicate that our system is sensitive to electrons even with energies of about 2·5 MeV or less. With the rates S_1S_2 and S_2 as obtained at the various depths underground we found that the chance coincidences accounted for approximately half the coincidences from the eighth channel (Δt = 7·76 to 15·32 μs) and almost all from the ninth (Δt = 15·32 to 30·52 μs) and the tenth (30·52 to 57·57 μs) channels. These, however, could be corrected for. The statistical errors in the corrections have a negligible effect on the final result. To give an example, we had to subtract (40 ± 6·3) chance coincidence counts recorded in the eighth, ninth and tenth channels when the total number of stopping muons recorded in all the gates was 376. The fractional error in the final result due to the subtraction procedure is, therefore, only about 1·9 % (= 6·3/336).

Having fixed the nominal voltage settings on the photomultipliers we observed, at the depth 96 hg cm^{-2}, as a function of voltage fed to the high voltage distribution panel: (1) the S_2^{ABC} and S_2^{DEF} chance coincidence rate; (2) the S_2 rate; (3) the S_1S_2 rate; and (4) the S_1S_2 delayed + S_2 coincidence rate (= stopping muon rate). These are all shown in figure 3. The observed S_1S_2 rate together with an assumed $\cos^2\theta$ type of zenith angle dependence of cosmic ray muon intensity enabled us to draw (5) the approximate omnidirectional muon rate through S_2. From (1), (2) and (5), we could determine (6) the S_2 rate due to radioactivity ((6) = (2) − (1) − (5)), which is shown in figure 3. The important thing to note in figure 3 is the fact that as long as the radioactivity counting rate in S_2 is about 1000 counts min^{-1} or more, our system is quite efficient in recording the stopping muon events. This is to be expected; for, the electron spectrum from muon decays which is of the form

$$N(x)\,dx = 2(3-2x)x^2\,dx$$

(x is the energy of an electron expressed as a fraction of its maximum possible energy) is peaked at high energies and as long as one is capable of seeing Compton electrons from gamma rays of the background radioactivity one is certainly efficient in detecting μ–e decays. This conclusion is shown in a quantitative way in figure 4 (obtained from the expression above) where we plotted the calculated efficiency to detect μ–e decays against the S_2 threshold in MeV. Even if we erred in the estimate of the threshold (shown by the broken line in figure 4) by a factor of 2, the detection efficiency is 99·9 %.

2.4. Nature of stopping particles being detected

As described in § 2.1, the experiment detects only the unstable charged particles. The experimentally measured pulse pair resolution of the electronics system is 60 ns; as a result, we cannot detect $\pi \rightarrow \mu$ or $K \rightarrow \mu$ decays. A typical decay time distribution, obtained at 96 hg cm^{-2}, is shown in figure 5, where we plotted on a semi-logarithmic

† This mild dependence of radioactivity counting rate on depth may be contrasted with the variation of the muon counting rate (given in the fourth row of the table 1) which decreases by a factor of nearly 200 in going from the first depth to the last.

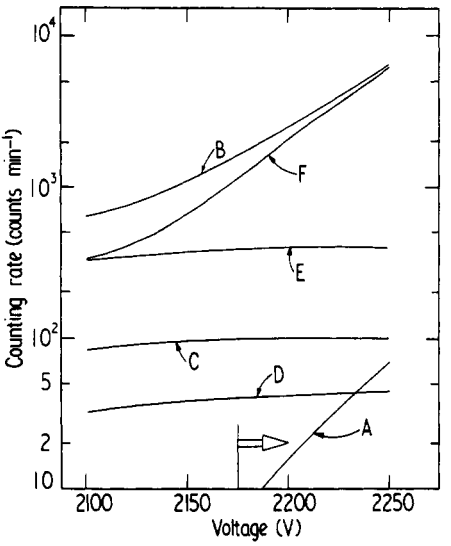

Figure 3. Various counting rates observed at 96 hg cm^{-2}, as a function of voltage input to the distribution panel. A, chance coincidence rate of S_2^{ABC} and S_2^{DEF}; B, S_2 rate; C, S_1S_2 rate; D, S_1S_2 delayed $+S_2$ coincidence (= stopping muon) rate; E, calculated approximate omnidirectional muon rate through S_2; and F, calculated S_2 rate due to radioactivity. The arrow at the bottom indicates the recommended region of operation.

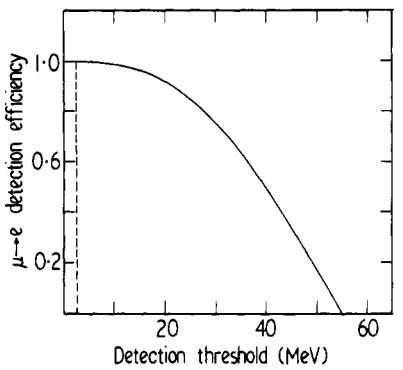

Figure 4. Calculated muon decay detection efficiency as a function of detection threshold.

graph the number of decays occurring after a time t, $N(>t)$, against time t (μs). A straight line of the type $N_0 \exp(-t/2{\cdot}16)$ fits the data well indicating that almost all the particles detected are muons†. If there is any other long lived (0·1 μs $< \tau <$ 25 μs) component besides the muon component, its amplitude is negligible. The decay time distribution curves obtained at the other two levels are also in agreement within errors with the hypothesis that the particles are all muons.

† The expected muon lifetime in the medium of the scintillator is calculated to be 2·13 μs taking into account the free muon lifetime (2·198 μs), the charge ratio of muons ($\mu^+/\mu^- = 1{\cdot}2$) and the chemical composition of the liquid scintillator (carbon:hydrogen = 9:1 by weight).

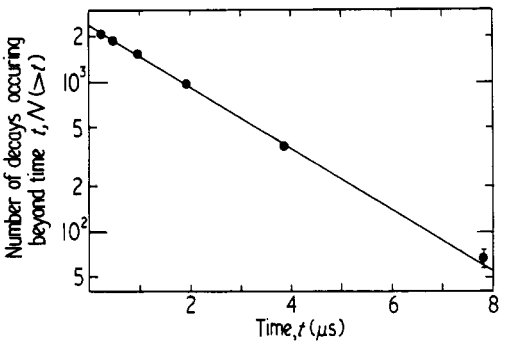

Figure 5. A semi-logarithmic plot of the number of decays occurring beyond t as a function of time t, observed at 96 hg cm^{-2}. The straight line is of the form $N_0 \exp(-t/2{\cdot}16)$ with t in microseconds.

2.5. Geometrical factor of the telescope and effective depths

The effective product of aperture (cm^2 sr) and thickness (g cm^{-2}) offered by the telescope to the low energy muon flux is calculated by dividing S_2 into slabs of 2 cm ($= 1{\cdot}746$ g cm^{-2} $= y$) thickness, treating S_1 and each slab of S_2 as a separate telescope and then summing the product for all such telescopes. In calculating this we assumed that the zenith angle dependence of low energy muons obeys a law of the type $I_\theta \propto \cos^n\theta$ where n is a parameter. First we calculated the differential aperture which is defined by

$$\frac{\mathrm{d}(A\Omega y)}{\mathrm{d}\theta} = \sum_{i=1}^{38} \cos^n\theta \frac{\mathrm{d}(A\Omega)i}{\mathrm{d}\theta} \frac{y}{\cos\theta}$$

where A is the effective area, Ω is the effective solid angle and $\{\mathrm{d}(A\Omega)i/\mathrm{d}\theta\}\,\mathrm{d}\theta$ is the geometrical factor (cm^2 sr) of the ith slab for the radiation incident in the zenith angular range θ to $\theta+\mathrm{d}\theta$ and y is the slab thickness in g cm^{-2}. The differential aperture is shown, as an example, in figure 6 for three values of n (1·6, 2·0 and 2·4). We then calculated the integral aperture defined by

$$A\Omega y = \sum_{i=1}^{38} \int_{\theta=0}^{\theta\,\max} \cos^n\theta \frac{\mathrm{d}(A\Omega)i}{\mathrm{d}\theta} \frac{y}{\cos\theta}\,\mathrm{d}\theta$$

which is the quantity (in cm^2 sr g cm^{-2}) offered by the telescope for a given value of n. Variation of this quantity with n is shown in figure 7. We have adopted, at all three depths, a value $n = 1{\cdot}9 \pm 0{\cdot}2$ which is close to the observed exponent for penetrating muons (see, for example, Achar *et al* 1965). It is evident from figure 7 that the aperture of our telescope and hence the fluxes obtained by us from the rates in this experiment do not depend sensitively on the value of n adopted.

We define the effective depth as the quantity $h \sec\alpha$ where h is the actual depth of the level measured vertically and α is the zenith angle where the differential distribution of the aperture reaches its maximum (see figure 6). Since $\alpha = 15{\cdot}5°$, the effective depth is 1·038 times the vertical depth in each case.

3. Results

3.1. Observations at the surface at Kolar Gold Fields

We just mention in passing that the stopping muon flux at the surface of the mines as

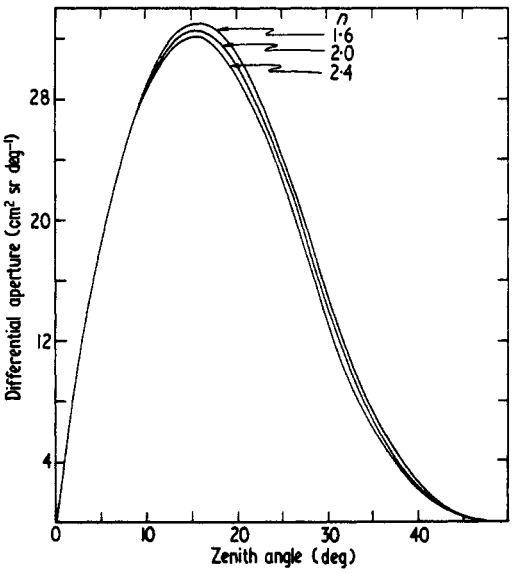

Figure 6. Differential aperture (in units of cm^2 sr deg^{-1}) of the telescope in figure 1 shown as a function of zenith angle (degrees) for three values of n, the exponent of the angular distribution of the incident radiation.

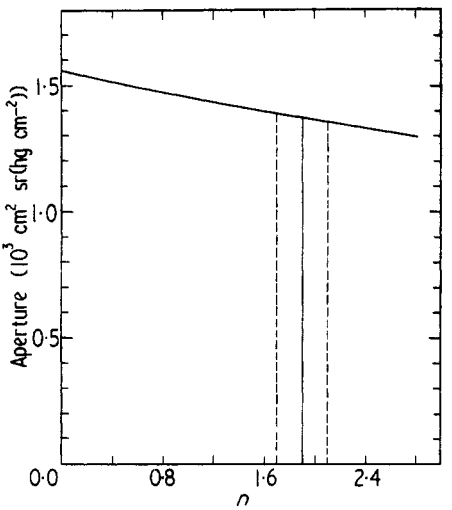

Figure 7. Integral aperture (in units of 10^3 cm^2 sr (hg cm^{-2})) offered by the telescope in figure 1 shown as a function of n, the exponent of the angular distribution of the incident radiation.

obtained by us is $(2{\cdot}62 \pm 0{\cdot}15) \times 10^{-4}$ muons $cm^{-2}\, s^{-1}\, sr^{-1}\, (100\ g\ cm^{-2})^{-1}$. This value is deduced from observed rate of stopping muons and the aperture calculated assuming a $\cos^{1{\cdot}9}\theta$ type of zenith angular dependence of the stopping muons.

3.2. Observations underground

The details of the observations are summarized in table 1. The first row lists the actual depths of the observation and the second, the effective depths arrived at by the procedure described in § 2.5. The errors in the stopping muon rates are statistical. The stopping muon rates have been corrected for chance coincidences as well as the loss of events in the time interval 0 to 55 ns which was not observed in our experiment. The calculation of the effective product of aperture and thickness appearing in the seventh row is described in § 2.5. The errors in the raw fluxes (eighth row) included both the statistical and systematic errors. The systematic errors arise mostly because our knowledge of the efficiency of the system for recording the muon decays is limited to an accuracy of $\pm 3\%$. The raw fluxes appearing in the eighth row have to be corrected for a number of effects which are mentioned in § 3.3.

Table 1. Details of the observations

Vertical depth (hg cm^{-2} below the top of atmosphere)	96 ± 2	417 ± 8	985 ± 20
Effective depth (hg cm^{-2} below the top of atmosphere)	100 ± 2	433 ± 8	1022 ± 20
S_2 rate (counts min^{-1})	~ 2400	~ 1000	~ 560
S_1S_2 rate (counts min^{-1})	$96 \pm 0{\cdot}2$	$2{\cdot}74 \pm 0{\cdot}04$	$0{\cdot}45 \pm 0{\cdot}007$
Duration of observation (h)	$47{\cdot}0 \pm 0{\cdot}03$	1687 ± 1	2729 ± 2
Stopping muon rate (counts h^{-1})	$(46{\cdot}6 \pm 1{\cdot}0)$	$(0{\cdot}44 \pm 0{\cdot}02)$	$(3{\cdot}8 \pm 0{\cdot}4) \times 10^{-2}$
Effective product of aperture and thickness (cm^2 sr (100 g cm^{-2}))	$1{\cdot}37 \times 10^3$	$1{\cdot}37 \times 10^3$	$1{\cdot}37 \times 10^3$
Vertical stopping muon flux, uncorrected (muons $cm^{-2}\, s^{-1}\, sr^{-1}$ $(100\ g\ cm^{-2})^{-1}$)	$(0{\cdot}94 \pm 0{\cdot}05) \times 10^{-5}$	$(9{\cdot}7 \pm 0{\cdot}6) \times 10^{-8}$	$(8{\cdot}5 \pm 0{\cdot}9) \times 10^{-9}$
Vertical flux of stopping muons, corrected (muons $cm^{-2}\, s^{-1}\, sr^{-1}$ (100 g cm^{-2} of rock)$^{-1}$)	$(7{\cdot}67 \pm 0{\cdot}4) \times 10^{-6}$	$(7{\cdot}9 \pm 0{\cdot}5) \times 10^{-8}$	$(6{\cdot}9 \pm 0{\cdot}7) \times 10^{-9}$
Vertical muon intensity (muons $cm^{-2}\, s^{-1}\, sr^{-1}$)	$(3{\cdot}70 \pm 0{\cdot}22) \times 10^{-4}$	$(1{\cdot}45 \pm 0{\cdot}10) \times 10^{-5}$	$(1{\cdot}5 \pm 0{\cdot}1) \times 10^{-6}$
The ratio R of the stopping muon flux to penetrating muon flux ((100 g cm^{-2}) of rock)	$(2{\cdot}07 \pm 0{\cdot}11) \times 10^{-2}$	$(5{\cdot}5 \pm 0{\cdot}3) \times 10^{-3}$	$(4{\cdot}6 \pm 0{\cdot}5) \times 10^{-3}$

3.3. Corrections

(i) Correction for the difference in the stopping powers of scintillator and rock: -10%.

(ii) Correction for the difference in the energy bites per g cm^{-2} of 100 g cm^{-2} of rock and 75 g cm^{-2} rock which is equivalent to 66·6 g cm^{-2} of liquid scintillator: -6%. The need for corrections (i) and (ii) arises in the context of *standardization* in reporting the fluxes to facilitate intercomparison of the results from various groups using different experimental arrangements. The standard unit we adopt in this paper (and urge the others to adopt) is muons cm^{-2} s^{-1} sr^{-1} (hg cm^{-2} of rock)$^{-1}$. In view of the existing discrepancy between the results reported by various groups, the importance of standardization can hardly be over emphasized.

(iii) Correction for the 'pillow effect' by which we mean the possibility of some of the muons stopping in the rock directly beneath S_2 and the decay electron travelling upward to enter and get registered in S_2 as a μ–e decay: -9%.

(iv) Correction for the 'edge effect' by which we mean the muon decays at the edges of S_2 and the decay electron leaves S_2 without getting registered in S_2 as a μ–e event: $+2{\cdot}3\%$.

(v) Correction for μ^- capture by the carbon atoms in the S_2 detector whose composition is 90% carbon and 10% hydrogen by weight: $+3{\cdot}1\%$. In calculating this, we had used the value 2·03 μs for the mean lifetime of μ^- in carbon as measured by Eckhause *et al* (1965).

Errors in the correction factors (i), (ii), (iii), (iv) and (v) discussed above, when expressed as fractions of correction factors themselves, are estimated to be $\pm 1{\cdot}5\%$, $\pm 1{\cdot}5\%$, $\pm 3\%$, $\pm 2\%$ and $\pm 0{\cdot}5\%$ respectively.

The fluxes of stopping muons corrected for all the effects listed above are given in the ninth row of the table. In the next row we have given the vertical intensities of muons. For the first depth, we have adopted a value deduced by us from the recently published accurate measurements on the sea level muon energy spectrum by Allkofer *et al* (1971) and for the second and third, values from the world survey of the depth–intensity relation by Menon and Ramana Murthy (1967). In the last row we have given the value of R which is the ratio of the flux of stopping muons to that of penetrating muons.

3.4. Additional observations at the depth 417 hg cm^{-2}

As mentioned earlier we assumed a $\cos^n\theta$ type of zenith angle distribution for low energy muons with $n = 1{\cdot}9 \pm 0{\cdot}2$. There were some suggestions (Keuffel 1971, Bergamasco *et al* 1972) that local production of low energy muons by high energy muons might make the zenith angular distribution of low energy muons flatter than what one assumed. To check this point we made three additional observations at the depth 417 hg cm^{-2}; these are described below.

3.4.1. S_2 trigger. During part of the observation the gates in our electronics (see figure 2) were opened by an S_2 pulse itself instead of by S_1S_2. By doing this we accepted stopping muons from all the zenith angles. Since the S_2 rate was much higher than the S_1S_2 rate, corrections due to chance coincidences were higher but calculable. After the corrections, the stopping muon rate is observed to be $(2{\cdot}42 \pm 0{\cdot}08)$ muons h^{-1}. One should compare this rate with the predicted† rates of $(8{\cdot}5 \pm 0{\cdot}5)$ and $(2{\cdot}8 \pm 0{\cdot}2)$ muons h^{-1} for $n = 0$

† In predicting these rates, it is assumed that the shape of the energy spectrum of stopping muons is not strongly dependent on the zenith angle.

(isotropic) and 1·9 respectively. These predictions were made on the basis of the flux values at 417 hg cm^{-2} given in the eighth row of the table and the amount of the liquid (386 kg) in S_2. Clearly the observation indicates that $n = 1{\cdot}9$ is nearer the truth and, if at all, it is slightly greater ($n = 2{\cdot}2$).

3.4.2. Thicker absorber in the path of muons. In the main experiment we employed a lead absorber which is 2·5 cm (= 28 g cm^{-2}) thick. Considering the thicknesses of the S_1 and S_2 scintillators and the absorber thickness, the apparatus was recording muons in the energy range 88 to 215 MeV. In a subsidiary experiment, we increased the thickness of the lead absorber to 12·7 cm (= 144 g cm^{-2}) shifting the response of the apparatus to the muon energy range 225 to 348 MeV. The raw flux value observed in the subsidiary experiment is $(8{\cdot}9 \pm 0{\cdot}9) \times 10^{-8}$ muons cm^{-2} s^{-1} sr^{-1} (hg cm^{-2})$^{-1}$ which is in good agreement with the value $(9{\cdot}7 \pm 0{\cdot}6) \times 10^{-8}$ muons cm^{-2} s^{-1} sr^{-1} (hg cm^{-2})$^{-1}$ from the main experiment. This agreement shows that the energy spectrum of low energy muons is flat up to energies of the order of 350 MeV, a feature that is to be expected if most or all the observed muons originate in the atmosphere and are slowed down in their passage to the level of observation. On the other hand the prediction for the energy spectrum of locally produced muons is model dependent and is not expected to be flat.

3.4.3. Low energy muons from very large zenith angles. To see if there is an unusually large flux of low energy muons from large zenith angles which one expects if there is profuse local production we placed a plastic scintillator S_1' to a side of S_2 as shown in the inset of figure 8 and triggered the recording system with $S_1'S_2$ coincidences instead of with S_1S_2. The dependence on the exponent of angular distribution of the product of aperture and thickness of the $S_1'S_2$ telescope (the quantity $A\Omega y$ explained in § 2.5)

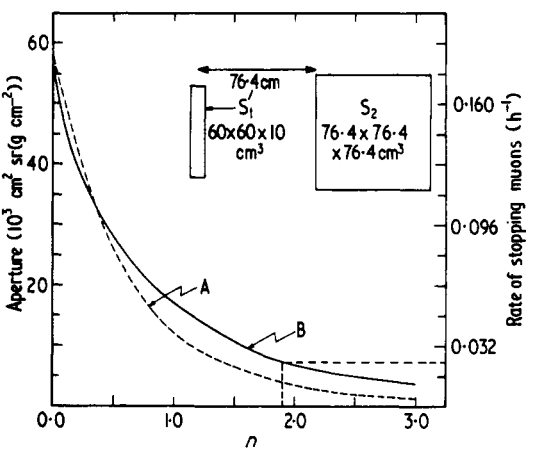

Figure 8. The inset shows the experimental arrangement employed for an additional observation at 417 hg cm^{-2}, described in § 3.4.3. Integral aperture (in units of 10^3 cm^2 sr (g cm^{-2})) offered by the telescope sketched in the inset shown as a function of n, the exponent of the angular distribution of the incident radiation. On the right, the ordinate is marked in terms of the expected rate of stopping muons. Curve A is based on a calculation without and curve B with a correction for Coulomb scattering of muons.

is shown in figure 8; curve A does not and curve B does take the scattering† of low energy muons into account. The stopping muon flux observed in the main experiment (row 8 of table 1) and the aperture shown in figure 8 allow us to label the ordinate in terms of stopping muon rate as shown on the right-hand side of figure 8. It is seen from figure 8 (curve B) that a value of $n = 1{\cdot}9 \pm 0{\cdot}2$ predicts a stopping muon rate of $(0{\cdot}024 \pm 0{\cdot}004)$ muons h^{-1} while the observed rate is $(0{\cdot}065 \pm 0{\cdot}018)$ muons h^{-1}. The difference $(0{\cdot}041 \pm 0{\cdot}018)$ muons h^{-1} may be a statistical fluctuation. If real, it is probably due to the local production of muons (see § 4 for a discussion) at such large zenith angles as defined by the $S_1'S_2$ geometry. One does not know the precise angular distribution of the locally produced muon component. If one assumes that it is isotropic, the difference between the observed and expected rates of stopping muons in this test implies that the fraction of locally produced muons among all those that stopped in the main experiment is less than $(12 \pm 5)\%$.

By the three additional observations mentioned in this section, we have learnt that: (i) the exponent of the angular distribution is not radically different from 2·0; (ii) the observations are consistent with a flat energy spectrum of low energy muons; and (iii) the fraction of locally produced muons at the depth 417 hg cm^{-2} is less than $(12 \pm 5)\%$.

4. Discussion

We have shown in figure 9 our results on the variation of R‡, the ratio of stopping to penetrating muon intensities, with depth along with those of the others. The points attributed to Baschiera *et al* (1970, 1971) are taken from the figures given by them and the ordinate values multiplied by 1·33 so as to correspond to our definition of R. Similarly the values reported by Short (1963), Kropp *et al* (1968)§, Reilly (1969), Barton *et al* (1970) and Elbert *et al* (1972) have all been recalculated by us to correspond to our definition of R and are shown in figure 9.

There are three known sources contributing to low energy muon fluxes underground. They are: (i) high energy muons produced in the terrestrial atmosphere, slowed down in the overlying rock and coming to rest in the medium under observation; (ii) low energy pions (decaying into muons) produced locally in the hadronic cascades initiated by high energy muons via photomeson production by the virtual or real photons associated with muons; and (iii) muons produced locally by high energy muonic neutrinos of the cosmic radiation. The absolute contribution from the last source is independent of depth and assumes significance only at depths greater than 7500 hg cm^{-2}, completely dominating the other two sources at depths of 8500 hg cm^{-2} or more (see, for example, Grupen *et al* 1972). However, we restrict the discussion here to depths less than 5000 hg cm^{-2} and therefore consider only the first two sources. Barton (1971), Grupen *et al* (1972) and Cassiday *et al* (1972) have calculated the contributions (i) and (ii) at various depths while Bergamasco *et al* (1972) calculated the expectation only for the depth

† Scattering of low energy muons does not appreciably alter the aperture values calculated (and shown in figure 7) for the main experiment for two reasons: (i) there is a 2·5 cm thick lead absorber in the path of the muons allowing only higher energy muons to be registered; and (ii) the telescope is narrow and vertically oriented.

‡ R is given in units of stopping muons $cm^{-2}\,s^{-1}\,sr^{-1}$ (hg cm^{-2} of rock)$^{-1}$ divided by penetrating muons $cm^{-2}\,s^{-1}\,sr^{-1}$, throughout this paper.

§ The depth at which these authors carried out their observations is not 1440 hg cm^{-2} as reported in their paper but 1568 hg cm^{-2} (private communication from W R Kropp).

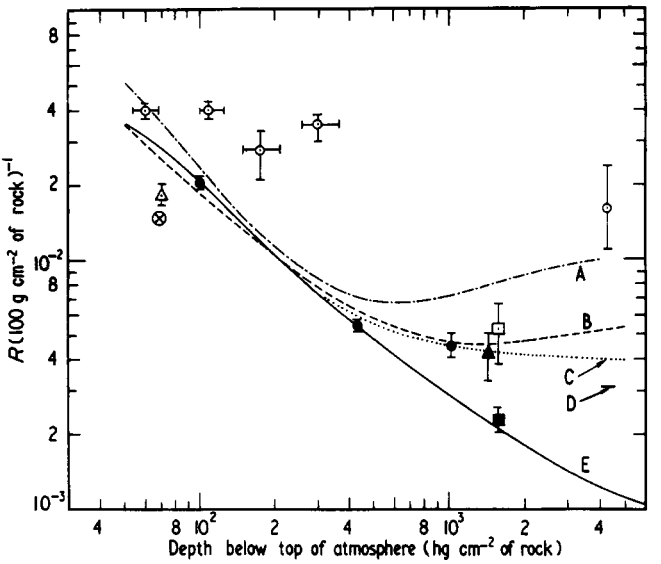

Figure 9. Variation of R, the ratio of the flux of stopping muons to that of penetrating muons as a function of depth from the top of atmosphere. The experimental points are: ⊗ Short; △ Barton *et al*; ⊙ Baschiera *et al*; □ Kropp *et al*; ■ Reilly; ▲ Elbert *et al*; and ● present experiment. The curves are the expected variations: A, Barton; B, Grupen *et al*; C, Cassiday *et al*; D Bergamasco *et al*; E, by us for the atmospheric muon component alone. Curves A to D include contributions from both atmospheric and locally produced muon components.

4270 hg cm^{-2} relevant to their experiment. These are all shown in figure 9 by the curves labelled A, B, C and D. We have also shown in figure 9 by curve E the contribution due to process (i) alone just to give an idea of its magnitude; we obtained this curve by differentiating the depth–intensity curve given by Menon and Ramana Murthy (1967). It should be emphasized that the curve E should be rather insensitive to slight differences in the previous 'world surveys' of vertical muon intensities at various depths; it is a ratio of stopping to penetrating muons and not an absolute intensity. Curve A is based on an admittedly approximate calculation. The virtual photon spectrum associated with muons and the photomeson production cross section are known well enough to expect a better agreement among curves B, C and D than what is obtained in figure 9. However, details such as angular distribution at emission, ionization loss of pions, and path lengths available for pion decays etc are important; this is perhaps the reason for the discrepancy between curves B, C, and D in figure 9.

First, we consider the measurements at shallow depths. It is seen from figure 9 that the R values and, therefore, the low energy muon fluxes obtained by Baschiera *et al* are much higher than those measured by us at a depth of 100 hg cm^{-2}. At least part of the discrepancy could be attributed, as pointed out by Bergamasco *et al*, to the differences in response of the two experimental arrangements to different angular distributions of stopping muons. The telescope in the present experiment is narrow and vertically oriented; conversion of rate to flux is therefore relatively insensitive to any error in the assumed value for the exponent n of the angular distribution. On the other hand, the apparatus of Baschiera *et al* has considerable aperture at large zenith angles and therefore conversion of rate to flux is strongly dependent on the value of n. Both the Coulomb scattering of low energy muons and the possible local production of muons tend to

make the exponent of the angular distribution of stopping muons less than 1·9, a value corresponding to that of penetrating muons. In the *extreme* case of low energy muons being isotropic ($n = 0$ instead of $n = 1{\cdot}9$) the error in conversion of counting rate to flux is only 14% in our experiment and could be as high as 200% in the case of an isotropic detector, such as the one employed by Baschiera *et al*. *We do not suggest* that n is as low as zero; for, we indeed have *indirectly* shown in § 3.4.1 that n is close to 2·0 at shallow depths. However, a *direct* measurement of the angular distribution of low energy muons is important in this context. We have an experiment in progress at 417 hg cm^{-2} to measure this.

We consider next the observations at depths of 1000 g cm^{-2} or more. Our observation at an effective depth of 1022 hg cm^{-2} along with those of Kropp *et al* and Elbert *et al* definitely establishes the existence of a locally produced muon component. Reilly's flux value at 1568 hg cm^{-2} is too low while that of Baschiera *et al* at 4270 hg cm^{-2} is too high. In Reilly's work, stopping muon events were *selected* on the basis that there should be a pulse in *only one* of the several scintillators surrounding the medium in which a muon stopped. Keuffel (1971) pointed out that such a selection criterion might veto the recording of locally generated muons as they would probably be associated with several other particles and, therefore, the flux reported by Reilly would correspond to the atmospheric muon component alone. While it is not clear as to what fraction of the locally produced component was not included by Reilly, it appears that he might have underestimated the flux. As shown by our observations discussed in § 3.4.3, the fraction of the locally produced muon component of the total seems to be $(12 \pm 5)\%$ or less for vertically oriented telescopes at 417 hg cm^{-2}. A comparison of our result at 1022 hg cm^{-2} with curve E (figure 9) indicates that this fraction goes up to $(37 \pm 7)\%$ at 1022 hg cm^{-2}. In terms of R, the locally produced muon component has a value $R_{\text{local}} = (1{\cdot}7 \pm 0{\cdot}3) \times 10^{-3}$ at 1022 hg cm^{-2} which is in good agreement with the calculations of Grupen *et al* (1972) and of Cassiday *et al* (1972). The average energy of muons arriving at any given depth increases almost linearly with depth up to depths of about 2000 hg cm^{-2} and remains constant at a value of 286 GeV at greater depths (see, for example, Craig *et al* 1968). Since the energy imparted to the hadronic cascades underground is a function of average muon energy, one expects R_{local} to increase with depth and then level off at a constant value of approximately $3{\cdot}0 \times 10^{-3}$. One expects, therefore, at the depth of 4280 hg cm^{-2}, R to be $4{\cdot}2 \times 10^{-3}$ representing the sum of contributions from the two sources: (i) atmospheric muons; and (ii) local production. Baschiera *et al* observe a value of $(1{\cdot}6^{+0{\cdot}8}_{-0{\cdot}5}) \times 10^{-2}$. Thus it appears that there is a discrepancy of a factor of 4. The discrepancy which is less than 2·5 standard deviations could just be due to a statistical fluctuation. Continued observations will settle this point.

5. Conclusions

We have measured in our experiment stopping muon fluxes of $(7{\cdot}67 \pm 0{\cdot}4) \times 10^{-6}$, $(7{\cdot}9 \pm 0{\cdot}5) \times 10^{-8}$ and $(6{\cdot}9 \pm 0{\cdot}7) \times 10^{-9}$ muons cm^{-2} s^{-1} sr^{-1} (100 g cm^{-2} of rock)$^{-1}$ at depth 96, 417 and 985 hg cm^{-2} respectively, measured from the top of the atmosphere. These flux values when divided by the vertical muon intensities (muons cm^{-2} s^{-1} sr^{-1}) at the corresponding depths yield ratios of $(2{\cdot}07 \pm 0{\cdot}11) \times 10^{-2}$, $(5{\cdot}5 \pm 0{\cdot}3) \times 10^{-3}$ and $(4{\cdot}6 \pm 0{\cdot}5) \times 10^{-3}$ respectively.

From our observations we have deduced that the locally produced muon flux constitutes a fraction of $(12 \pm 5)\%$ or less and $(37 \pm 7)\%$ of the total for vertically oriented

telescopes at depths 417 and 985 hg cm^{-2} respectively. Our observations on the total low energy muon fluxes are in good agreement with the calculations of Grupen *et al* (1972) and of Cassiday *et al* (1972).

The observations of Baschiera *et al* (1970, 1971) on stopping muon fluxes at a depth of 4280 hg cm^{-2} appear to be anomalously too high. However, the number of events observed by them is too small to rule out statistical fluctuations. If borne out by larger statistics, the results of Baschiera *et al* are very important since they imply the existence of new processes. Continued observations of the rate as well as the angular distribution of the stopping muons will help to improve the significance of their result.

Acknowledgments

We are grateful to Professor B V Sreekantan for his comments. Our thanks are due to Mr A D Ranpura for his assistance in the experiment and to Mr A V John for his computational help. We are grateful to the Managing Director and staff of Bharat Gold Mines Limited (Kolar Gold Fields) for their cooperation.

References

Achar C V, Narasimham V S, Ramana Murthy P V, Creed D R, Pattison J B M and Wolfendale A W 1965 *Proc. Phys. Soc.* **86** 1305–15

Allkofer O C, Carstensen K and Dau W D 1971 *Phys. Lett.* **36B** 425–7

Barton J C 1971 *Proc. 12th Int. Conf. on Cosmic Rays, Hobart* vol 7 (Hobart: University of Tasmania) pp 2825–8

Barton J C, Betts J P and Pourgourides C M 1970 *Proc. 6th Interam. Sem. on Cosmic Rays, La Paz, Bolivia* vol 4 (University of San Andreas) pp 1029–36

Baschiera B, Bergamasco L, Castagnoli C and Picchi P 1970 *Lett. Nuovo Cim.* **4** 121–3

—— 1971 *Lett. Nuovo Cim.* **1** 961–6

Bergamasco L, Castagnoli C, D'Ettorre Piazzoli B and Picchi P 1972 *Lett. Nuovo Cim.* **4** 39–42

Bhat P N and Ramana Murthy P V 1971 *Proc. 12th Int. Conf. on Cosmic Rays, Hobart* vol 7 (Hobart: University of Tasmania) pp 2829–35

—— 1972 *Lett. Nuovo Cim.* **4** 543–9

—— 1973 *Lett. Nuovo Cim.* submitted for publication

Cassiday G L, Keuffel J W and Thompson J A 1972 preprint

Craig R, Osborne J L, Wolfendale A W and Young E C M 1968 *J. Phys.* A: *Gen. Phys.* **1** 61–71

Eckhause M, Siegal R T and Welsh R E 1965 *Nucl. Phys.* **81** 575–83

Elbert J W, Keuffel J W and Thompson J A 1972 *Phys. Rev. Lett.* **29** 1270–4

George E P 1952 *Progress in Elementary Particle and Cosmic Ray Physics* ed J G Wilson and S A Wothuysen vol 1 (Amsterdam: North-Holland) pp 393–452

Grupen C, Wolfendale A W and Young E C M 1972 *Nuovo Cim.* B **10** 144–54

Keuffel J W 1971 *Lett. Nuovo Cim.* **2** 669–73

Kropp W R, Reines F and Woods Jr R M 1968 *Phys. Rev. Lett.* **20** 1451–2

Menon M G K and Ramana Murthy P V 1967 *Progress in Elementary Particle and Cosmic Ray Physics* ed J G Wilson and S A Wothuysen vol 9 (Amsterdam: North-Holland) pp 163–243

Reilly T D 1969 *PhD Thesis* Case Western Reserve University

Short A M 1963 *Proc. Phys. Soc.* **81** 841–5